HIFAN 1318
LBNL – 54920

Induction Accelerators for the Phase Rotator System

Lou Reginato, Simon Yu, Dave Vanecek

Lawrence Berkeley National Laboratory

INTRODUCTION

The principle of magnetic induction has been applied to the acceleration of high current beams in betatrons and a variety of induction accelerators. [1] The linear induction accelerator (LIA) consists of a simple nonresonant structure where the drive voltage is applied to an axially symmetric gap that encloses a toroidal ferromagnetic material. The change in flux in the magnetic core induces an axial electric field that provides particle acceleration. This simple nonresonant (low Q) structure acts as a single turn transformer that can accelerate from hundreds of amperes to tens of kiloamperes, basically only limited by the drive impedance. The LIA is typically a low gradient structure that can provide acceleration fields of varying shapes and time durations from tens of nanoseconds to several microseconds. The efficiency of the LIA depends on the beam current and can exceed 50% if the beam current exceeds the magnetization current required by the ferromagnetic material. The acceleration voltage available is simply given by the expression V=A dB/dt. Hence, for a given cross section of material, the beam pulse duration influences the energy gain. Furthermore, a premium is put on minimizing the diameter, which impacts the total weight or cost of the magnetic material. The diameter doubly impacts the cost of the LIA since the power (cost) to drive the cores is proportional to the volume as well.

The waveform requirements during the beam pulse makes it necessary to make provisions in the pulsing system to maintain the desired dB/dt during the useful part of the acceleration cycle. This is typically done two ways, by using the final stage of the pulse forming network (PFN) and by the pulse compensation network usually in close proximity of the acceleration cell.

The choice of magnetic materials will be made by testing various materials both ferromagnetic and ferrimagnetic. These materials will include the nickel-iron, silicon steel amorphous and various types of ferrites not only to determine the properties that are essential in this application but the energy losses in the magnetization process which directly impact the cost.

Accelerator Waveforms

The parameter and pulse format from Study 1 and Study 2 have evolved toward considerably improved physics performance and less demanding accelerator waveforms avoiding the need for multipulsing.

The Feasibility Study 2 of the Neutrino Factory and Muon Collider have resulted in the architecture on Fig. 1 and the acceleration waveforms shown on Fig. 2. The waveforms for Induction 1(Ind1), Induction 2(Ind2) and Induction 3 (Ind3) are all-unipolar. That is, the

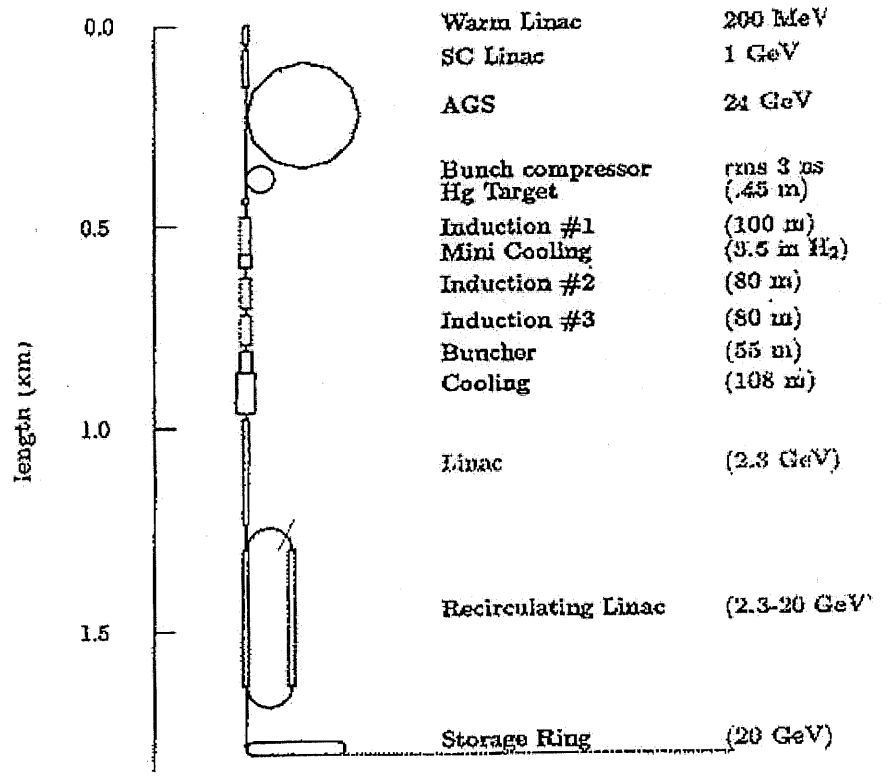

Fig.1- Neutrino Factory and Muon Collider Specifications

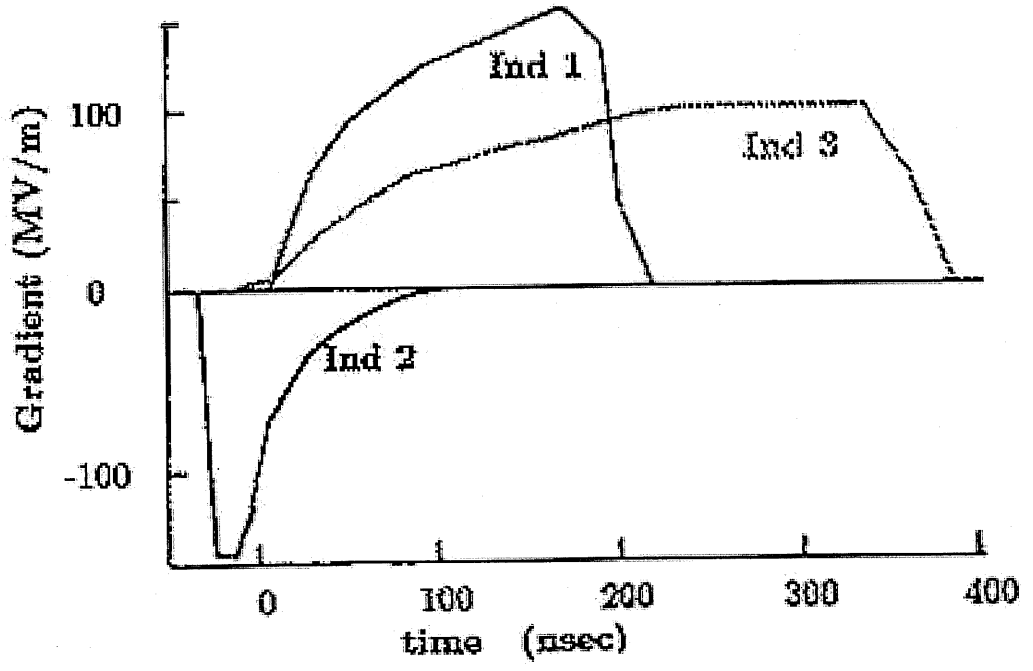

Fig. 2- Acceleration Waveforms for Induction 1,2 and 3

acceleration (deceleration) waveforms do not reverse in polarity during the beam pulse. Although Ind2 and Ind3 were initially combined during one design version of study 2, it became preferable for technical reasons and to reduce the risk factors to separate the two functions with a small penalty in economics. A combined Ind 2 and Ind 3 would require the application of "branched magnetics" to achieve two waveforms that are independently controllable in shape and timing. The branched magnetics approach could lead to a 5-10% cost savings but at more risk since this approach has only been applied to small benchtop prototypes but not to presently operating induction accelerators. This approach will be reviewed in Appendix B.

Magnetic Material

A number of induction accelerators have been constructed in the past that cover the pulse duration of the three induction accelerators required by the Neutrino Factory and Muon Collider. None of these accelerators, however, have gradients and energy gains that are as high. To satisfy the requirements in an economically feasible design, it is imperative to choose a magnetic material and a pulsing system, which minimizes the cost but still achieves the reliability and performance required.

In the past two decades, great strides have been made in the development of a magnetic material which is replacing all previous ones in the 60Hz power industry because of its low loss, ease of manufacturing and low cost. Several alloys are made in ribbon form by rapidly quenching a stream of molten material on a cold rotating drum. The ribbon thickness is typically 25μm and can be of any width from 5 to 20cm. Because the ribbon is so thin and has higher resistivity than other ferromagnetic materials, it is directly applicable to short pulse applications. In short pulse applications where the rate of magnetization (dB/dt) is very high, tens of volts are generated between the layers of ribbon when it is wound into a toroid. Thin insulation such as 2-4μm mylar must be used between layers to insure that the ribbon layers are sufficiently insulated to hold off the voltage generated.

The soft magnetic properties can be improved by annealing. This procedure, although well below the crystallization temperature, embrittles the material to make it nearly impossible to wind into a toroid. Annealing can be done after winding if the insulating material between layers has a high melting point but when mylar is used annealing is not an option. Coatings have been developed which allow annealing after winding but at the present time they are not fully developed and do not hold off sufficient voltage per turn. Because the losses at high magnetization rates are almost entirely due to the eddy current losses, very little is lost in using the material "as cast" or unannealed as it is planned for this application.

In order to choose the appropriate alloy of this amorphous material it is important to measure the properties such as flux swing (delta B) and magnetization (delta H) at the appropriate pulse duration or magnetization rate (dB/dt). Fig. 3 shows the losses in Joules/m^3 at different rates of magnetization. It can be seen that above one Tesla/microsecond that the losses increase linearly with magnetization rate. From Fig. 3 it appears that the lowest loss material is the alloy 2705M with the lowest delta B of about 1.4 Tesla while the highest loss material is the 2605CO with a delta B of about 3.3 Tesla. The optimum material is selected by considering the delta B (Tesla), the losses (Joules/m^3) and the cost ($/kg). Two alloys which are not plotted on this chart (Fig. 3) are the 2605SA1 used exclusively in the 60Hz power industry and the 2605S3A which is used in pulse transformer applications. The SA1 material offers the potential for greatest savings since it

is mass produced for the power industry but has not been investigated as thoroughly as the SC or S3A materials at the very short pulse regime. For this exercise the SC alloy is chosen since it has been used recently in an induction accelerator for radiography at the Los Alamos National Laboratory and extensive technical and cost data exist. The S3A also offers a good choice since it has also been used extensively in the AVLIS program at the Lawrence Livermore National Laboratory. The SA1 alloy will be further investigated in the near future since, as mentioned previously, it offers the greatest possibility for more cost savings.

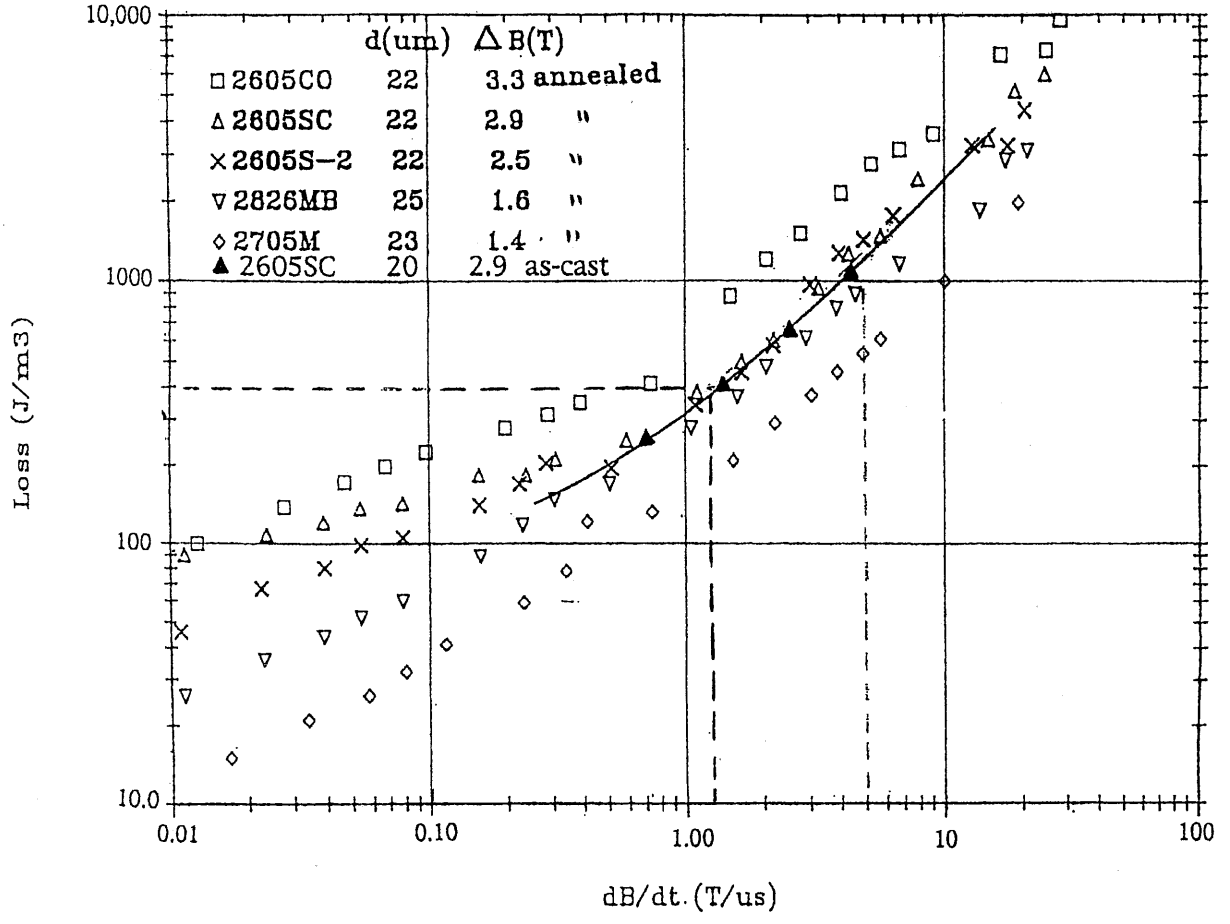

Fig.3-Losses (J/m3) of several amorphous alloys as a function of magnetization rate (dB/dt).

Induction 1 Cell

From the specifications of RB Palmer et al. shown on Fig. 1, Induction 1 is 100m in length and has the acceleration waveform shown on Fig. 2. The waveform has a full width half max (FWHM) of about 180 ns with an approximately exponential rise time of 100 ns and a fast fall time. The significant portion of the acceleration cycle is during the rise time while the fall time is not important. In fact, the fall time will be longer than indicated by the waveform since the energy stored in the cell inductance will decay with a time constant t=L/R of the drive circuit. The L/R of the fall time will be similar to the rise-time, hence, the FWHM will be about 250 ns. Since a one-meter section will have to allow axial space for the cryogenic feed lines and for

vacuum pumping, the maximum allowable space for the core is 712mm. In order to obtain the lowest cost possible for the amorphous material, it is required that the alloy be cast in widths of 101.6mm (4") or greater. The manufacturing limits, therefore, dictate a maximum number of cells that is a multiple of 101.6mm. That number, of course, is seven since that adds up to a total of 712mm.

From the gradient we now have a basis for calculating the cross-sectional area of the magnetic material for Induction 1. From V=A(dB/dt)(PF) we can calculate the delta R knowing the delta Z and the packing factor (PF=.75). From previous data, the hysterisis loop for the two alloys 2605SC and 2605S3A are shown on Fig. 4.

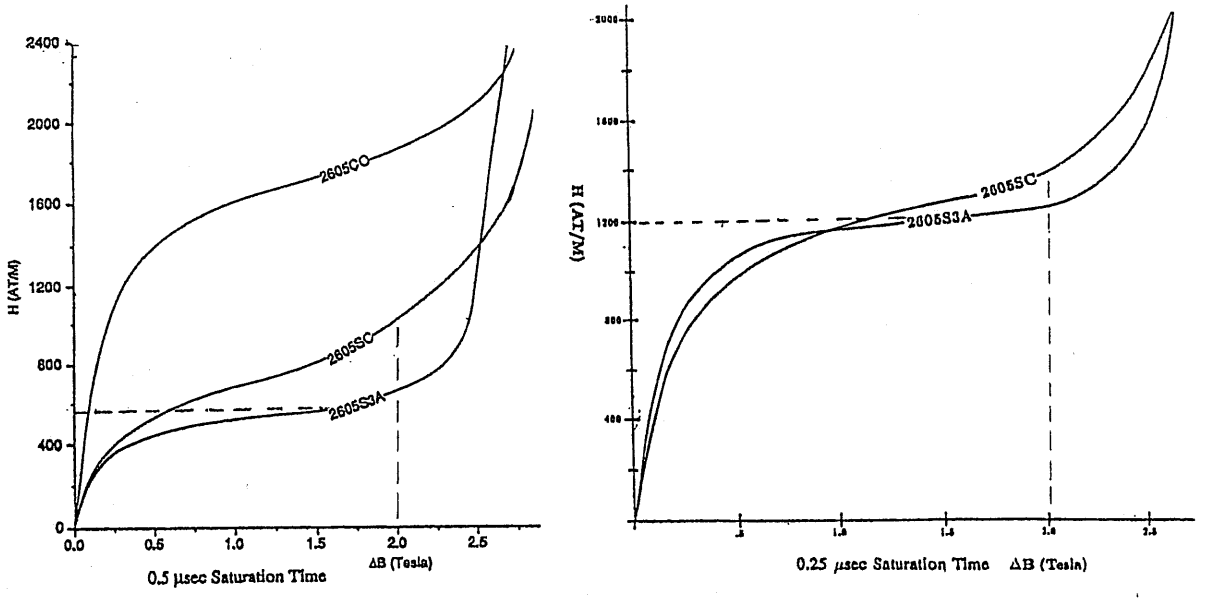

Fig. 4-Hysterisis for 2605 SC and 2605S3A at two different magnetization rates.

Although the total flux swing to saturation is over 2.5 Tesla, the actual working flux swing (delta B) is chosen at 2.0T so that the pulse generator drives into a more linear load. The required voltage for each of the seven cells that constitute one meter of acceleration is 214.3kV. The actual cross sectional area $A= V \Delta t / \Delta B$ (PF) or $A=(r_2 - r_1)$ (.1016) = (214.310^3) (25010^{-9}) / (2.0) (.75) $r_2 - r_1$ = .352m. The inside radius of the core is set by the outside radius of the superconducting solenoid at a minimum of 400mm. Preliminary calculations of the leakage flux at the solenoid gaps indicates that this flux which is orthogonal to the magnetization flux can be of the order of a few thousand gauss at the 400mm radius. From previous accelerator tests such as the Advanced Test Accelerator (ATA) and the Dual Axis Radiographic Hydro Test (DARHT) accelerators indicate that this is acceptable but this issue should be investigated further with laboratory tests to insure that the flux swing of the induction cell is not reduced by this stray flux. To be on the safe side, the inside radius of the actual amorphous material is therefore set at 500mm. The magnetizing current and all the losses can now be calculated. $\Delta H = \Delta I/\pi d$ where d is the average diameter or $d=r_2 + r_1$ =1.35m. From Fig. 4 for the 0.25μs saturation time we find that the magnetizing force ΔH=1200A/m or ΔI=5,087A and the losses $U=V \bullet \Delta I \bullet \Delta t$ or $U=(214.310^3)(5.08710^3)(25010^{-9})$ = 272.5 Joules/cell. The magnetic material volume including

the Mylar insulation $V=\pi (r^2_2 - r^2_1)(\Delta Z)$ or $V=.151m^3$ and with a packing factor of 0.75 the actual volume of amorphous material is $0.131m^3$ and at 7290 kg/m^3 it weighs 825kg. The core losses could have been calculated by looking at Fig. 3 which shows that the losses per cubic meter at a magnetization rate $dB/dt=2.0T/.25\mu s$, $2,000J/m^3$ for a total of 262J or slightly lower than above. The previous loss calculations determine the drive power required by the pulse generator for one cell or for seven cells $P=7V\cdot I$ with V=214.3kV, I=35.6 kA, P=7.63GW and the impedance Z=V/I=6.0 ohms.

Fig.5- (a) Cross section of a single cell with compensation network
(b) Cross section of a two meter section

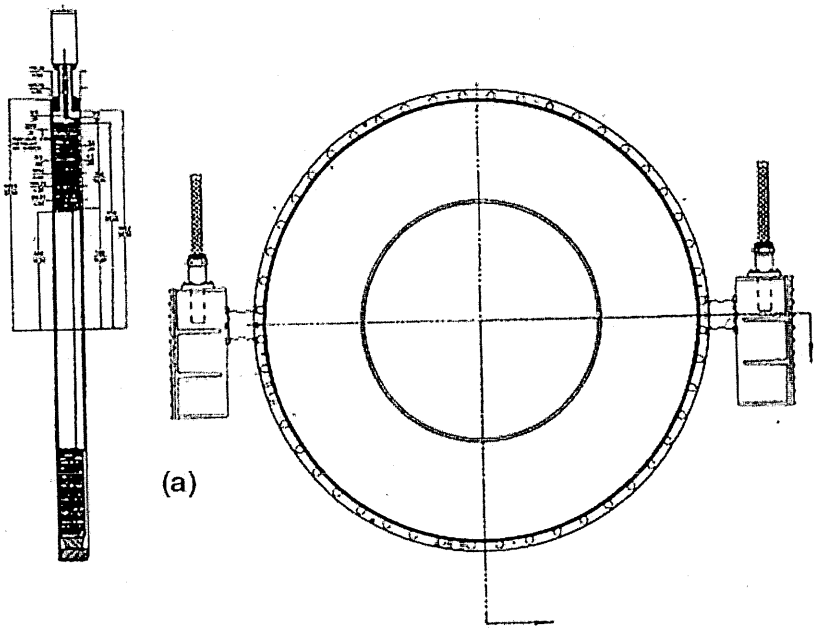

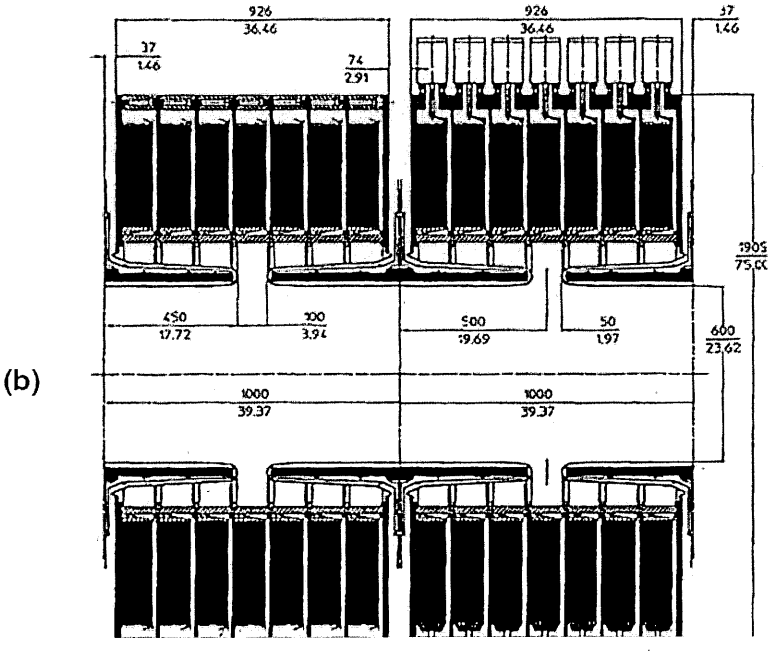

High Voltage Design of Cell

Fig. 5 shows a cross section of the induction cell. The cell is driven by two high voltage cables at 180°. The high voltage cables plug into two connections of the type used on the DARHT accelerator and part of the compensation network box. The acceleration gap is 1cm and is oil filled. From Fig. 6, which shows the voltage breakdown in oil for different pulse durations and surface areas, it appears that the safety factors are more than adequate, that is, the actual breakdown is about twice the operating voltage. The highest voltage stress occurs at the outside radius of the core where one half of the driving voltage appears from each side of the core to ground. The insulation is achieved using about ten layers of 50μm mylar with oil impregnation.

Fig. 6- Short Pulse Voltage Breakdown in Oil

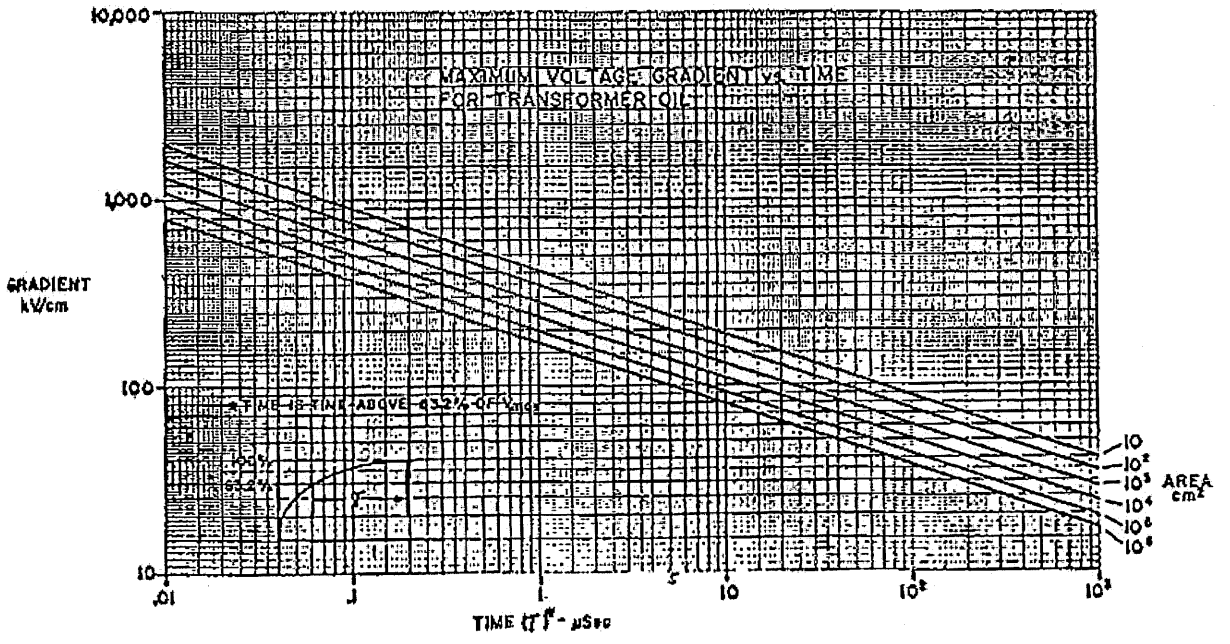

The interface oil-to-vacuum insulator is designed so that on the vacuum side the field lines form a 30° or greater angle with the insulator to achieve the highest possible voltage holding. The empirical curve shown on Fig. 7 shows the voltage flash over for different angles. For our design, the maximum surface gradient on the insulator is nearly one order of magnitude lower.

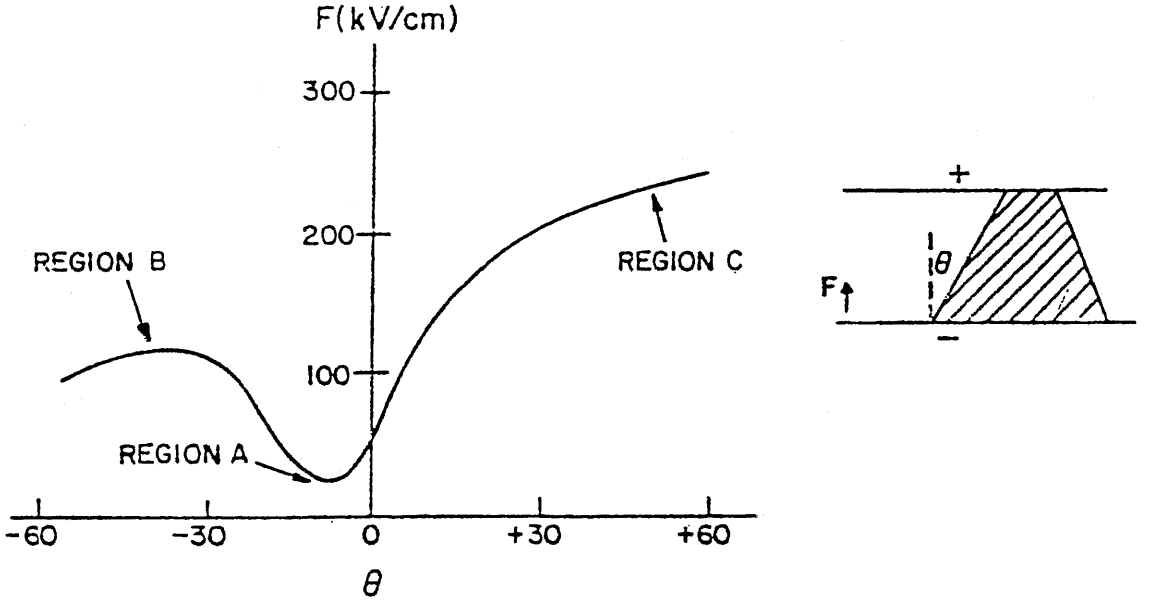

Fig. 7 – Flashover Voltage with a 30ns pulse for different cone angles

The highest voltage gradient occurs between the solenoid housings. This spacing is 100mm and the radius is 30mm and using the cylindrical geometry the maximum gradient is about 150-200 kV/cm. Fig 8 shows field emission at 200ns for different types of surfaces and it appears that for a standard electropolished stainless steel surface this is marginally acceptable and the surfaces should be greened or the gradient should be reduced somewhat, by redesigning the nose pieces.

Induction 2 Cell

From the specifications shown on Fig. 2 for Ind2, the deceleration pulse has an unspecified rise time (from zero to a negative value) and a fall time (from a negative value back to zero) which is the significant portion of the beam acceleration time of about 50 ns.

Induction accelerators with pulse durations of less than 100 ns have traditionally used nickel-zinc ferrites as the magnetic material of choice. The choice of Ni-Zn ferrites was the appropriate choice a decade or two ago when the last short pulse induction accelerator was built since the amorphous materials were not of a very high quality and inexpensive as they are today. The choice of ferrites also was logical if one compares their losses to those of amorphous materials at saturation times of 50ns. One can see from Fig. 9 that if full saturation is achieved in 50 ns, the losses for ferrites (CMD 5005) are about 800 J/m^3 while the losses for amorphous materials (2605SC) are about one order of magnitude higher. Even though the flux swing for amorphous materials is five times greater than those of the ferrites the losses are more than one order of magnitude greater (at full saturation). However, since the cost of ferrites has quadrupled in the past two decades while the cost of amorphous materials has decreased considerably, it is imperative to take another look at using amorphous materials of the same cross-section (volume) as the ferrites since this would mean that the flux swing would be much lower than that at full saturation as would be the magnetization rates, hence, the losses. In order to make the best comparison, a design was made of both the ferrites and the amorphous materials. Using the standard 101.6mm width (w) and a delta B (from Fig 10) of 0.5 Tesla for the ferrite CMD 5005 then the area $A=w\,(r_2 - r_1) = V\Delta t/\Delta B$. From Fig. 2 the significant part of the acceleration waveform is the fall time while the rise time is unspecified and will be determined by the pulse generators. Because of the large gap capacitance and the impedance of the pulse generator, the rise time will be nearly the same as the fall time so that the FWHM will be about 100 ns.

Using 100 ns as FWHM or Δt and the per cell voltage V=188kV then the outside radius r_2=870mm. From Fig 10 the hystesisis curve for CMD 5005 indicates that ΔH=1000A/m and the losses will be 500 J/m^3. The ferrite volume $V=\pi\,(r_2^2 - r_1^2)$ $W=.162m^3$ which will result in 81J of losses per cell requiring a drive current I=4.3kA. Using the same cross sectional area but applying the amorphous materials, one can now find the losses. Because the packing factor of the amorphous material will be 0.75 instead of unity the flux swing will be .667T and the magnetization rate $dB/dt = 6.67T/\mu s$ (i.e 100ns saturation). From Fig. 3 we see that the losses for 2605 SC will be about 1400 J/m^3. The total losses, U, for the amorphous material will be $U=(1400J/m^3)(.162m^3)(.75)$ or U=170J/cell. The losses using the amorphous material are about twice as high as those of the ferrites and, therefore, the cost of the pulse generator will be that much greater. The economics, however, still favor the amorphous material because its cost is about one fourth of that of the ferrites. Even though the pulse generator doubles in cost, the net result is a saving of about 10%.

It is interesting to note that the design for Induction 2 is nearly identical to Induction 1, that is, r_2=.85m for Ind.1 and r_2=.87m for Ind. 2 so in actuality for manufacturing and design cost saving

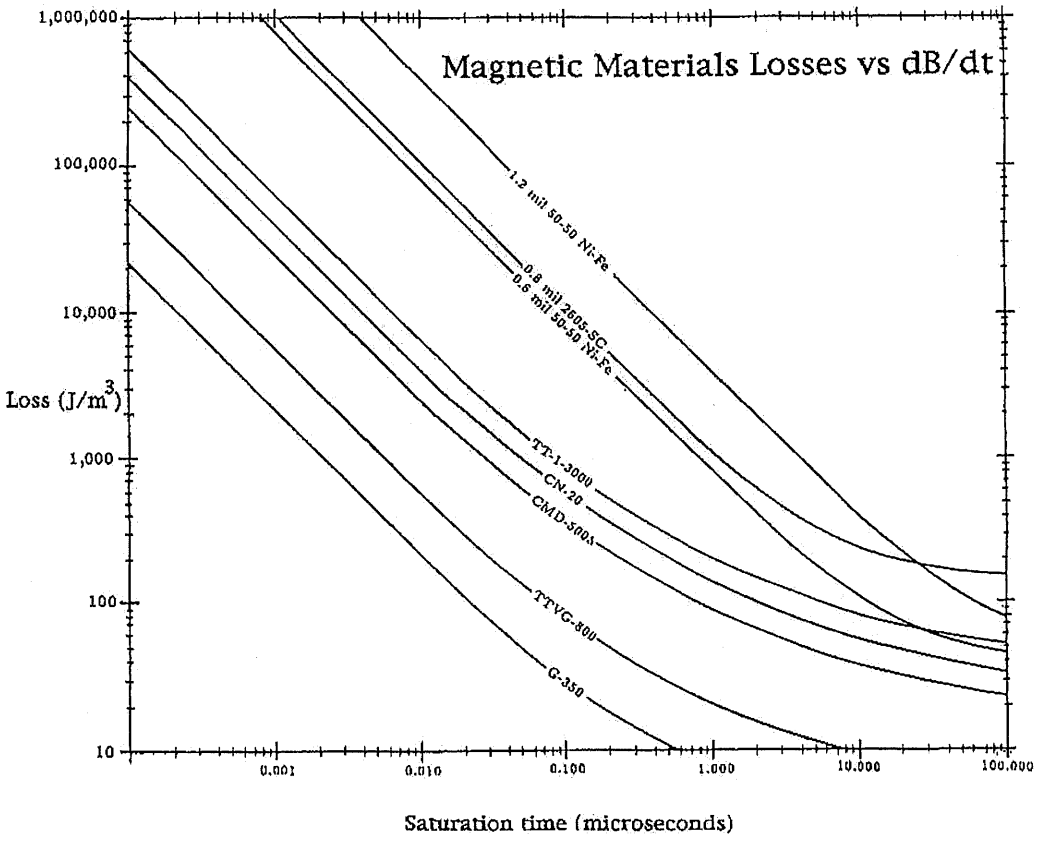

Fig.9- Magnetic Materials losses for different saturation times

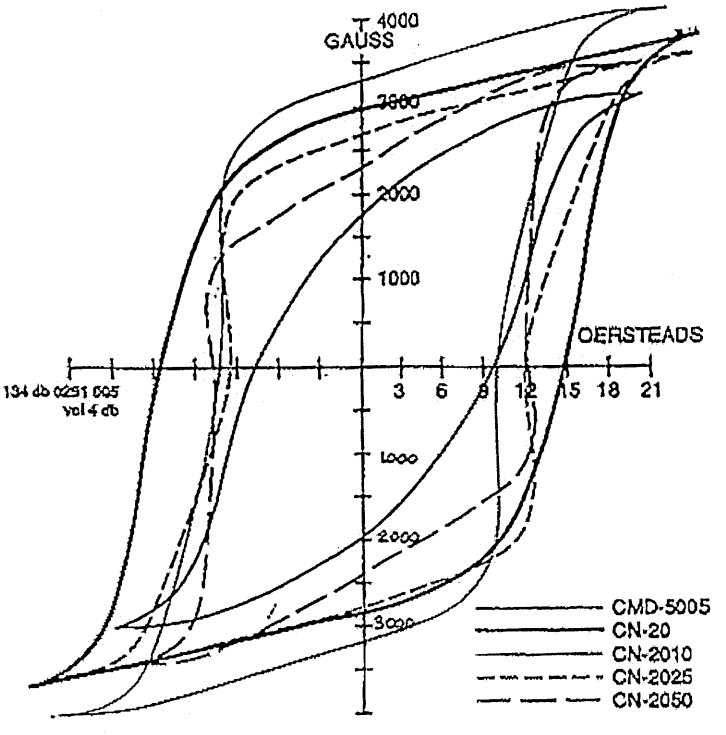

Hysteresis curves measured at τ_{set} = 50 ns

Fig. 10 –Hysterisis Curves for various ferrites

the two cells can be identical. Since Induction 2 is a decelerating gradient, the induction cells for this accelerator are simply installed rotated 180° from those of Induction 1.

Induction 3 Cell

Applying the same arguments used in the design of Induction 1, the FWHM for Induction 3 is 380 ns and the acceleration voltage V=143kV. The outside radius of this cell can now be calculated from $V \cdot \Delta t = A \cdot \Delta B$ (PF). The magnetization rate for this cell will be lower since the saturation time is longer. For the same delta B as in Induction 1 or ΔB=2.0T, the dB/dt = 5.26T/μs and the magnetization will be the average between the two cases shown on Fig. 4 or ΔH=900A/m. Applying these parameters to the design of Induction 3, from $w(r_2 - r_1) = V\Delta t/\Delta B$(PF) we get r_2 = 857mm. The magnetizing current is $I=\pi H (r_2 + r_1)$ =3.84kA and the cell losses $U=V \cdot I \cdot \Delta t = (143 10^3)(3.84 10^3)(380 10^{-9})$ =209 Joules. The volume of material $V=\pi(r^2_2 - r^2_1)(w)$ = .155m^3 and the weight (W) with a PF=.75 W=846kg. Table I Summarizes the three induction accelerators and all the important parameters.

TABLE 1.

Accel	MV/ m	Length m	Δt ns	IR m	OR m	Vol. Cell ms	Wgt. Cell Kg	ΔB Tesla	ΔH A/m	Volts kV	Amps kA	Energy J	Total Wgt Tonnes
Ind 1	1.5	100	250	.5	.85	.151	826	2.0	1200	214	5.09	273	578
Ind 2	1.5	80	100	.5	.87	.162	886	0.67	2100	188	9.05	170	496
Ind 3	1.0	80	380	.5	.86	.155	846	2.0	900	143	3.84	209	474

It is evident from Table I that the three induction accelerators can be identical as far as induction cells are concerned. Each pulsing system will, of course, be different.

The amorphous alloy used in this study was not optimized but was chosen simply because the most reliable information exists for the short pulse applications and the most accurate cost data was available from a recent induction accelerator constructed at LANL for radiography. It is very likely that the alloy being mass produced for the power industry, 2605SA1, can be substituted for the 2605 SC. The SA1 material has great potential for cost reduction since it is mass produced in such very large quantities. We will pursue testing samples of SA1 in the near future and will begin negotiations with the scientific staff at Honeywell (had bought Alllied Signal) to explore making the material in thinner ribbon and less expensive than the SC material.

Pulsing System

The Induction Accelerators 1, 2 and 3 are driven by pulse generators with output voltages from 100-200 kV, currents in the tens of kiloamperes at pulse duration from 50ns to 300ns. The peak power levels exceed one gigawatt and except for spark gaps, no switches exist which are capable of operating reliably at the required repetition rates and power levels. Since spark gaps

are not acceptable, the only option available is the nonlinear magnetic pulse compression modulator.

The use of saturable reactors for generating very high peak power levels was described by Melville[2] in 1951. The basic principle behind magnetic pulse switching is to use the large changes in permeability exhibited by saturating ferri-(ferro) magnetic materials to produce large changes in impedance. The standard technique for capitalizing on this behavior is shown on Fig.11. By using the multiple stages shown it is possible to compress a pulse of relatively low power and long duration into a pulse of very high peak power and very short duration maintaining the same energy (except for a small core loss) per pulse. This is exactly the technique which allows us to use available thyratrons or solid state devices to initiate the pulse and then pulse compress it to the desirable peak power levels.

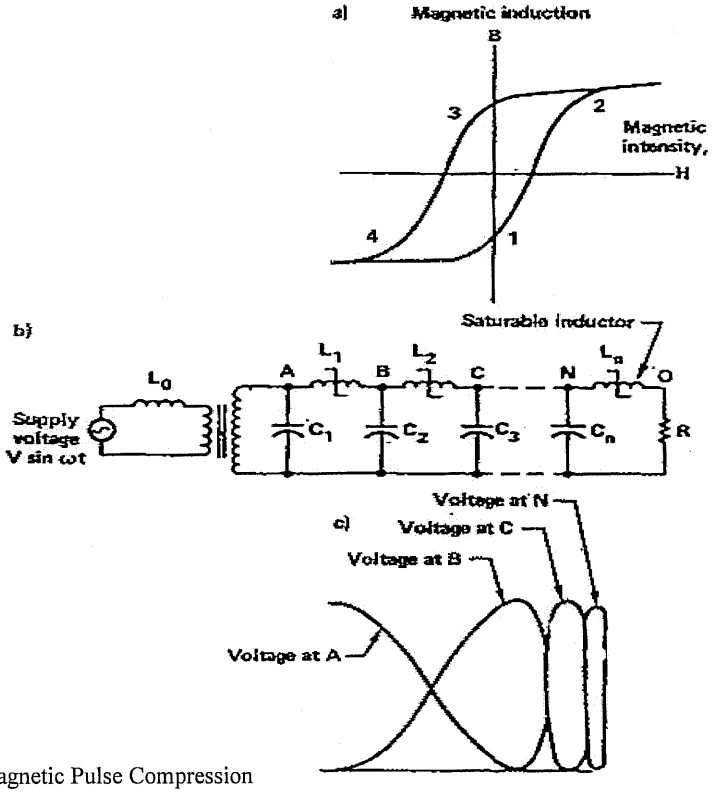

Fig. 11 – Principle of Magnetic Pulse Compression

The principle of operation of the magnetic pulse compressor has been covered extensively in the literature but is briefly described here for continuity. Capcitor C1 charges through inductance L_0 until inductance L_1 saturates, becoming much less than L_0. Once this happens, C_2 will begin to charge from C_1 through L_{1sat}, but since L_{1sat} is much less than L_0, C_2 charges more rapidly than C_1 did. This process continues through the successive stages until C_n discharges into the load through $L_{n\ sat}$.

To make this process efficient, we design each of these successive stages so that saturation occurs at the peak of the voltage waveform. Segment 1 to 2 in the hysteresis loop of Fig. 11 is the active or high-permeability region during which the inductor impedes current flow; the leveling off of the curve at point 2, reached at the peak of the voltage waveform, indicates core saturation when the inductor achieves a low impedance. During segment 2 to 4, the core is reset to its original state, ready for the next cycle.

Induction 1 Pulse compressor

The requirement for induction 1 is to generate an acceleration pulse shape and gradient shown on Fig 1 and 2. Each accelerator cell previously described must produce a voltage of 214 kV and after the beam traverses 700 of these cells it will have gained 150 MV of energy. From Table I, the necessary drive current for one cell is 5.09KA for a duration full width half maximum (FWHM) of 250 ns. As previously mentioned, no switches exist which can produce this type of pulse directly so by investigating the optimum operating voltage and current of the switches, the required stages of compression will be decided. Since Thyristors have limits in di/dt of several kiloamperes/microsecond and voltage limits of a few kilovolts it can be seen that a large number of them in series and parallel combination will be required. Thyratrons also have limits in di/dt and voltage but these limits are at least one order of magnitude greater than thyristors. Thyristors have practically unlimited life while the thyratrons have an operating life of the order of 20,000 hours. Even taking into consideration replacement costs, the thyratrons offer a simpler and more economical pulse compression system (fewer stages).

For technical and economic reasons, the pulse compression system is designed to drive one

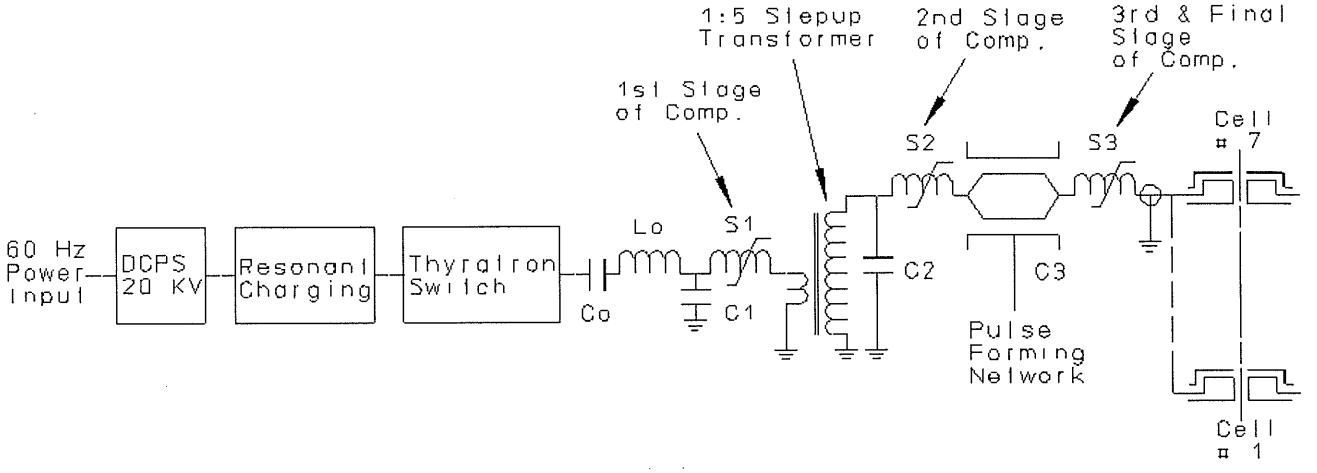

Fig. 12- Simplified Diagram of Ind. 1 7-Cell Pulse Generator

meter or all seven induction cells. The total energy required will be U=273x7=1,911 Joules plus the additional losses incurred in the pulse compression scheme. The 500 Joule pulse compression system (Fig. 13)designed to replace the Advanced Test Accelerator spark gaps achieved efficiencies greater than 90%. Allowing for 5% losses in the thyratron switches, 5% losses in the resonant charging and 5% in the power supply, the total input energy per pulse is 2,548 Joules and at 15Hz average repetition rate the total power for seven cells W=38.2 kW. The total power for Induction 1, $W_t = 3.82$ MW.

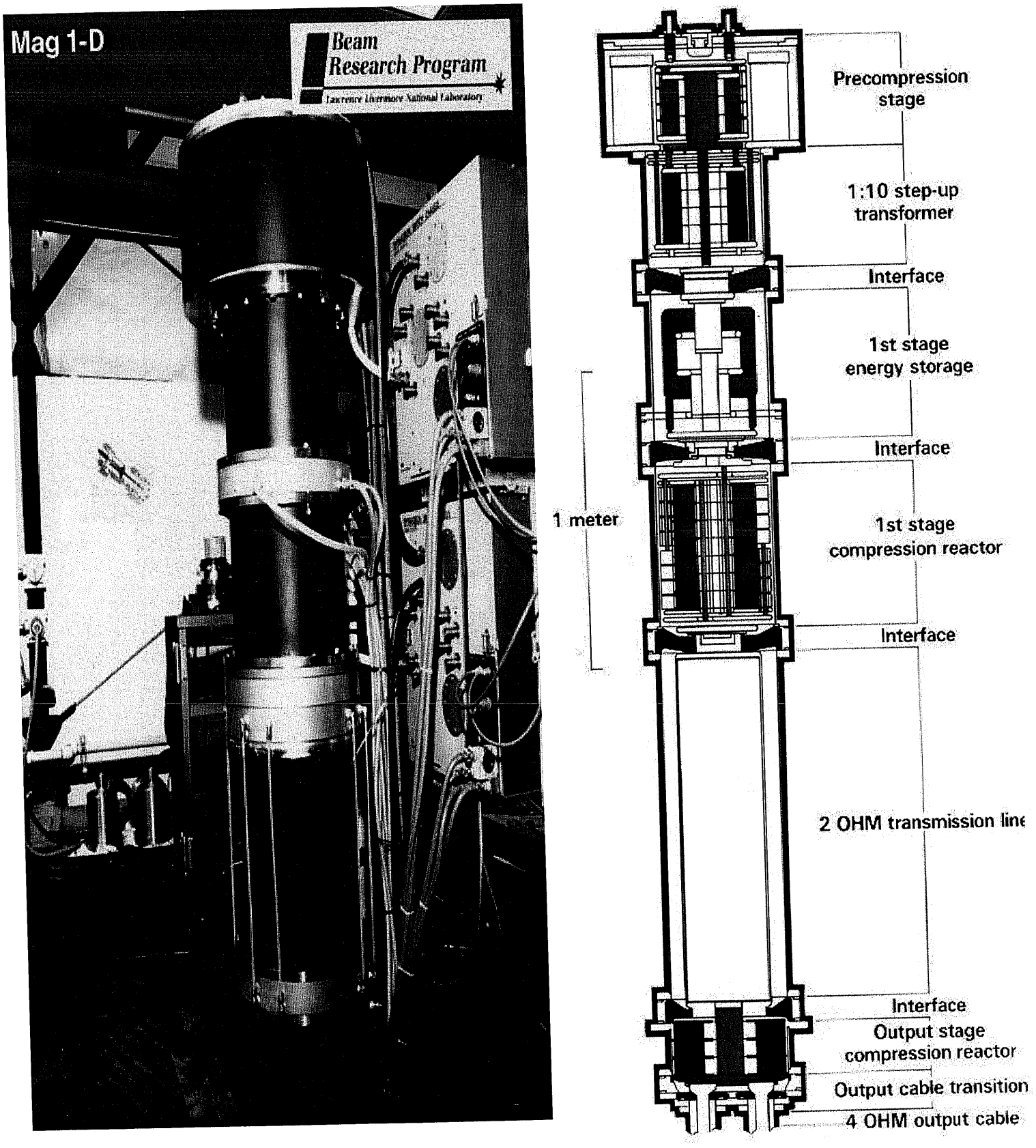

Fig.13- 500 Joule Mag 1-D Magnetic Pulse Compression Modulator Driving the ETA II Accelerator

7-Cell Pulse Generator

Fig. 12 shows a simplified diagrams of the pulse generator which will drive 7 cells with a voltage pulse of 214kV, 35.6 kA and a pulse duration FWHM=250ns. The resonant charger intitiates the sequence by charging capacitor C_0 to 2xVdcps or 30-40 kV. The charging current through C_0 will have the effect of partially resetting the first stage compression and the step up transformer. The reset of the other stages and the induction cells will be done by a separate pulse generator just prior to initiating the pulse sequence. The optimum saturable reactor is obtained by designing a time compression of about 3:1 and with three stages the total compression will be about 27:1. The thyratron switch will discharge C_0 in about 6.8μs. As the magnetic switch, S1, saturates, it will discharge C1 into the transformer primary with a time period of 2.25μs. This primary voltage of 30kV will be stepped up to 428kV and charge C2 with a l-Coswt waveform. The magnetic switch S2 will be designed to saturate at the peak of this waveform which will charge the pulse forming network in 750ns. Finally, the saturable reactor S3 will switch the PFN energy at the peak of that waveform delivering the energy to the seven cells. The desired waveform will be achieved by tailoring the temporal impedance of the PFN to that of the nonlinear load of the cells. Further waveform tailoring is done using series inductors and compensation network (R&C) in the boxes on each side of the cells.

The total energy that must be switched by the thyratrons include the system losses and amounts to 2548 Joules. This energy is stored in capacitor Co=5.66μF and is switched into C1 through inductor L1=.828μH with a series impedance Z_0=.382 ohms.

This results in a peak half sine wave current of 28kA for a peak power of 2.3GW. Several options in thyratrons are available. The highest continuous power thyratrons are the ceramic envelope units while the glass envelope units are capable of nearly as high a peak power with low average power capability. Since the average power is moderate (38 kW) the appropriate choice for technical and economic reasons are the glass envelope units. In order to carry the 78kA peak current, twelve parallel devices will have to be used. To insure current sharing, each thyratron will switch its own capacitor which is Co/12=.47μF.

Except for thyratron replacement every 20,000 hours or more of operation, the pulse compression systems should be maintenance free since all components are passive devices.

Induction 2 Pulse Compressor

The pulse duration for the Ind. 2 accelerator has a FWHM=100ns. Assuming an additional 5% loss since the pulse compression system has to go one step further, the total input energy for seven cells U=1,700 Joules and at 15Hz will result in a power requirement of 25.5kW. The total power requirement for Induction 1 is 2.04MW. The pulse duration for Ind. 2 is 100ns FWHM. The shorter pulse duration would dictate an additional stage of pulse compression on the system described for Ind. 1. However, since the energy for Ind. 2 is 68% of Ind. 1, it is possible to achieve the shorter pulse duration with the same number of stages simply initiating the compression process by starting with a shorter pulse duration. The design of each stage, of couse,

will be different and the transformer will have a step-up of 12:1. For Ind 2 the Co=3.78μF and the compression for three stages will be 36 for an initial discharge time to 3.6μs with L_0 = .347μH and Z_0 =.303 ohms. The peak current required of the twelve thratrons will be 99kA or 8.25kA each.

Induction 3 Pulse Compressor

The pulse duration for Ind. 3 is 380ns FWHM. A pulse compression similar to Ind 1 with three stages will be used. The step-up transformer will have a step-up of about 10:1 and the three saturable reactors will be similar to Ind. 1. The energy at the imput U=1951 Joule and at 15Hz average repitition rate, the input power per seven cells is 29.3 kW and the total imput power W_t=2.34MW. With the input energy of 1951 Joules, the capacitor Co=4.34μF and with an initial discharge time to =10.3μs the inductor L_0=2.46μH and the series impedance Z_0=.753 ohms which results in a peak current of 40kA.

The total power required for Induction 1,2 and 3 at 15Hz average repetition rate will be 8.2MW including the efficiency of 90% for the DC charging power supplies, the total 60Hz power requirement will be very nearly 9MW.

TABLE II Energy and Power Requirements

Ind. Accel	Length (m)	Pulser Enegy (J/m)	Total Energy (kJ)	Total Power @ 15Hz (kW)
Induction 1	100	2,548	254.8	4,247
Induction 2	80	1,190	126.9	2,115
Induction 3	80	1951	156.1	2,602
Total Power required from Grid				8,964kW

Mechanical Systems

In order to achieve the desired gradient for the three induction accelerators, the induction cells are driven by the pulsing system in units of seven, hence, mechanically these cells are likewise assembled into one module by bolting together seven cells.

The individual cores are assembled at the Honeywell plant in Conway, South Carolina. The mandrel on which the amorphous material is wound on supports the complete core and an additional support cradle is included on the OD of the core to insure that there is no sagging (Fig. 14). As specified under electrical requirements, the cores are wound with 101.6 mm wide ribbon with 3μm Mylar

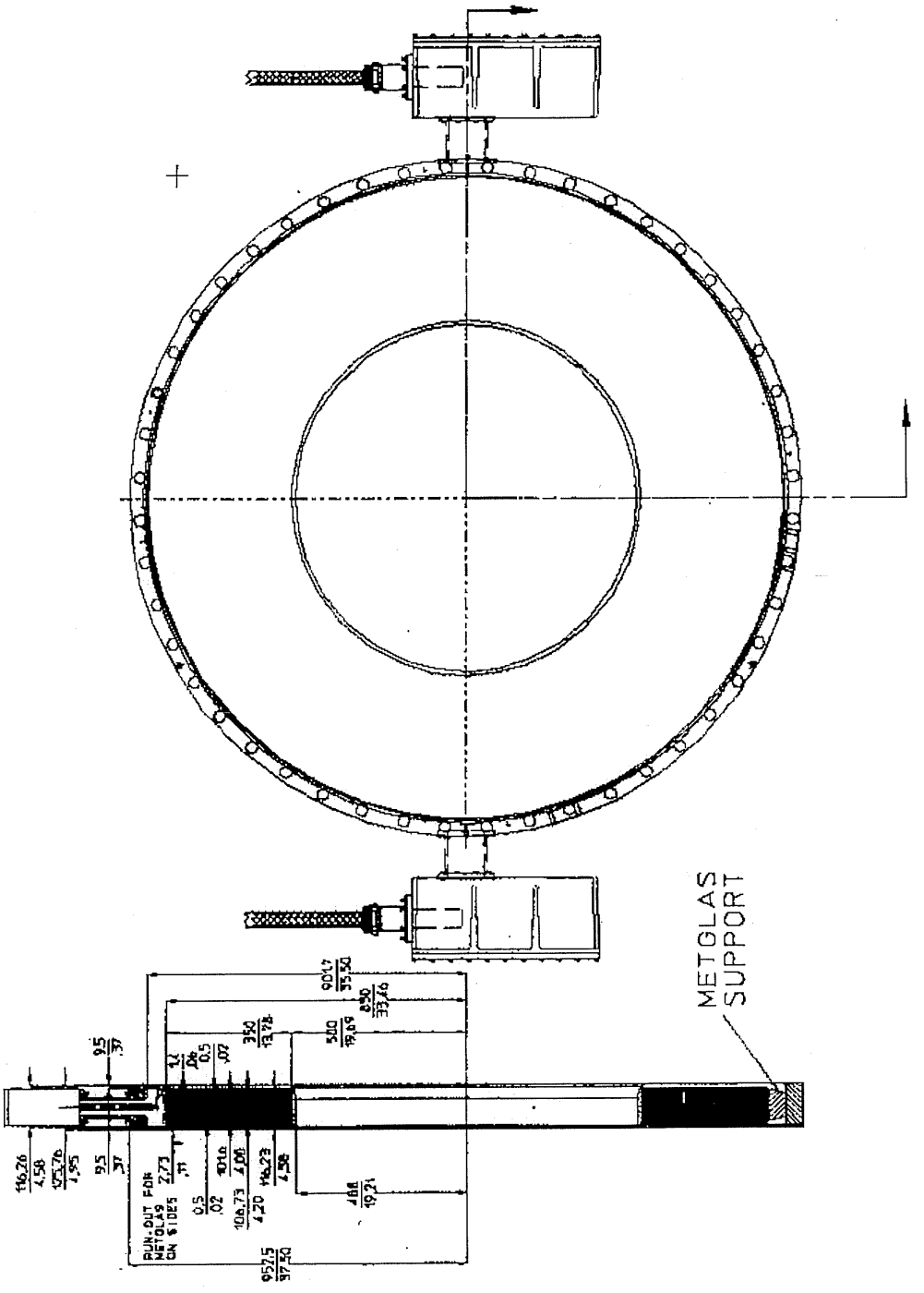

Fig. 14 – Metglas Single Cell Assembly

between layers and protruding 3mm beyond the ribbon. From previous experience, the complete core has a packing factor (PF) of about 75%.

The high voltage insulator, which is the oil to vacuum interface, is assembled in seven sections for each module and voltage grading of each section is provided by making contact with the appropriate cell. Each section will have a gradient ring which will insure that the field lines will enter the insulator at an angle of about 30° to insure maximum voltage holding (Fig. 7). The seven section insulator is made of "Mykroy/Mycalex and will be glued together as in the DARHT accelerator (Fig. 15).

The induction module housing is fabricated and assembled using seven large rings which will be fastened together by outside fixtures similar to those used in the Relativistic Two-beam Accelerator (RTA) at LBNL. The whole module is supported on the OD from these rings by a six-strut support system (Fig.16). The support system allows for excellent alignment of each module with respect to each other and beam position.

The vacuum system will consist of turbo pumps and cryopumps located every 5-10 modules. This placement will be finalized after detail calculations of the vacuum requirements. These pumps will be connected to a roughing line along side of the accelerator. Beam position and total current diagnostics will also be located at the pump out station.

Each module with its downstream cryo magnet is assembled and aligned prior to installation in the beam line. After installation in the beam line, the module is aligned and the vacuum seal is fastened.

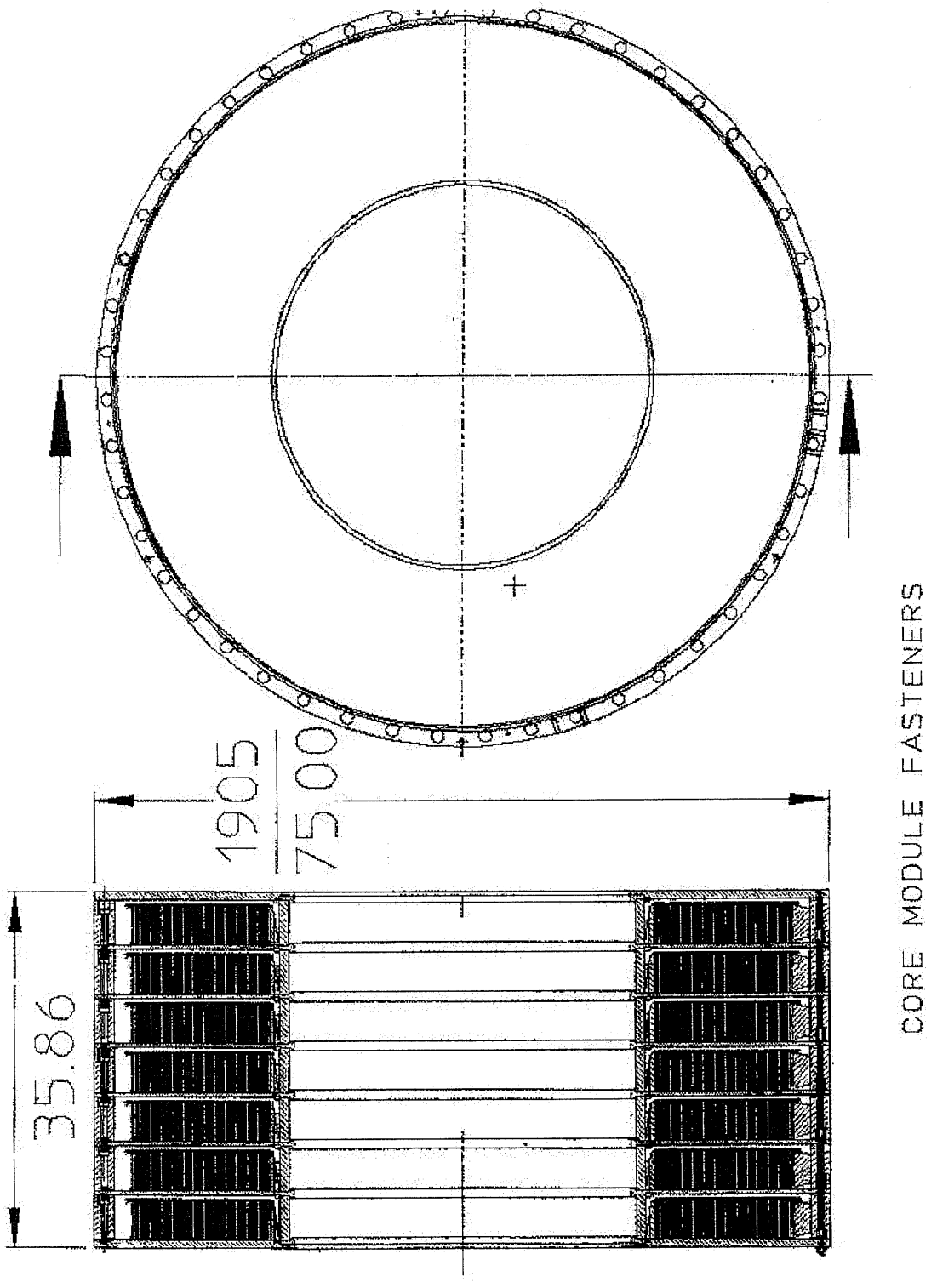

Fig.15-Seven Cells housing which forms one Accelerator module

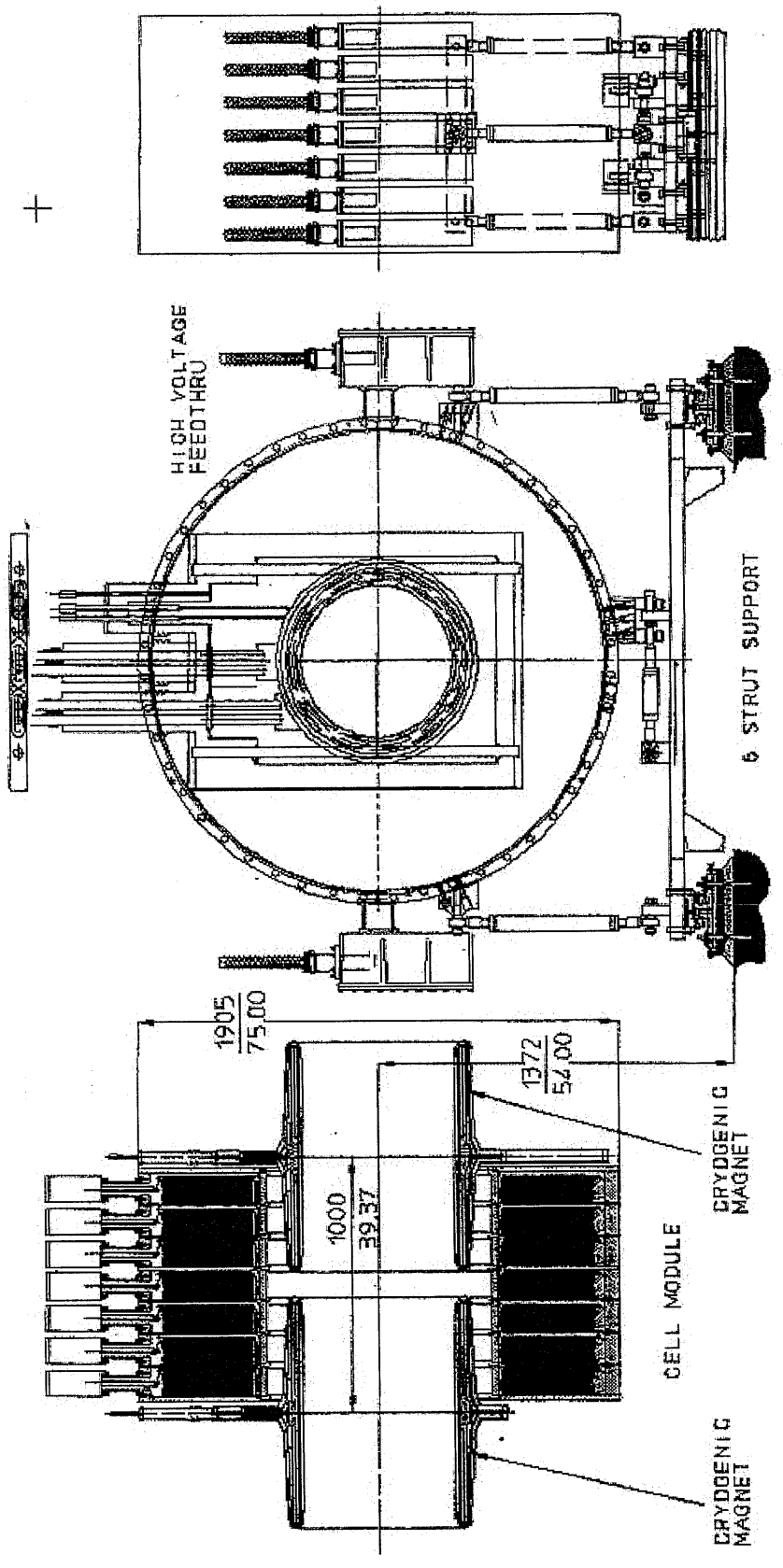

Fig. 16-Six strut module support system

Summary

The design of the induction accelerators required for the Neutrino Factory and Muon Collider are based on similar designs of previously constructed accelerators. There is no equivalent experience with induction accelerators having pulse durations and gradients the same as Induction 1, 2 and 3. Furthermore, the reliability and lifetime expectancy of 10^{10} shots dictated the use of a drive technology, magnetic pulse compression, which is considerably more expensive than the standard or direct drive approach of the DARHT accelerator. Before a conceptual design is made, full scale prototypes should be designed and tested in order to confirm the waveform requirements and the actual cost.

Very large quantities of amorphous material are required (1500 Tonnes) and considerable savings can be realized if a less expensive alloy such as 2605SA1 is used. This alloy must, however, be thoroughly tested to insure that it has sufficiently low loss to not increase the pulsers drive requirements. Considerable testing should be done of the SA1 alloy at the magnetization rates (pulse saturation) required by Induction 1, 2 and 3. From the Heavy Ion Fusion Program, LBL has the capability of winding its own test cores if the raw material is made available (Fig. 17).

The superconducting solenoids have dictated an inside radius for the cores which is much larger than previously constructed accelerators. This design leads to very large cores and very large power losses since the energy scales as the volume (weight) of the magnetic material. Studies should be carried out to insure that the stray fields from the super conducting solenoids do not adversely affect the magnetic cores flux swing and their inside radius should be reduced as much as possible.

Since the magnetic material properties are fundamental to the design of three accelerators, testing should begin as soon as possible to achieve the optimum solution.

REFERENCES

1. N.C. Christofilos "High Current Linear Induction Accelerators for Electrons" The Review of Scientific Instruments. Vol. 35, No. 7- July 1964.

2. W.S. Melville "The Use of Saturable Reactors as Discharge Devices for Pulse Generators" The Institution of Electrical Engineers. Vol. 98, Part III, No. 53. May 1951.

3. D.L. Birx "An Investigation Into the Repetition Rate Limitations of Magnetic Switches" UCRL 87278, Feb. 10, 1982, Lawrence Livermore National Laboratory

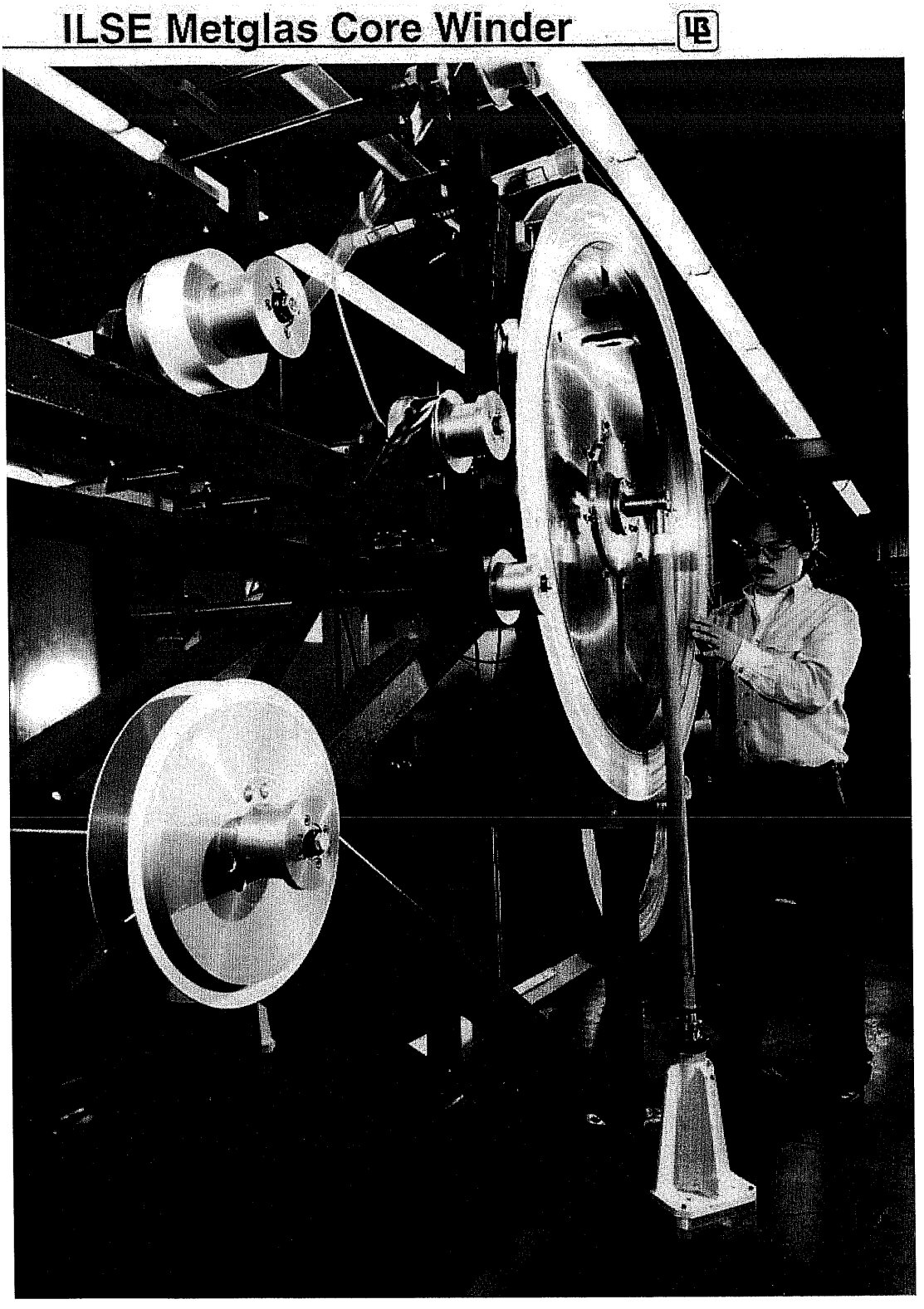

Fig. 17- A prototype induction core being wound at LBNL.

APPENDIX A

Cost Estimating

The cost estimates presented for the electrical systems of Induction 1, 2 and 3 were derived by a couple of methods. The first method took magnetic pulse compression generators built for previous accelerators (Fig. 13) and deriving a cost per Joule or cost per watt figure. The cost per Joule or cost/watt is not linear with size, that is, the dollars/Joule for a 10x driver is more like 5x the cost of 1x. therefore, this rule was applied.

In the second method, a detail design was made of the driver and each individual component was costed including the fabrication and assembly time. The two methods yielded fairly close results and the average was chosen as the final cost.

There are two other mitigating factors that will reduce the cost when very large quantities are involved. One factor is referred to as the "learning curve" and the other is the "mass production" curve. The learning curve is the phenomenon whereby, as the number of units increases, the assembly becomes more efficient and the amount of time for performing the repetitive task decreases.

Each of the Induction Accelerators will require of the order of 100 drivers or units to be assembled. Since these drivers are somewhat different for each accelerator, to total number of units or assembly cycles is taken as 100 rather than 300. From the approximate learning curve of Fig. 18, the cost of assembly for each of the drivers will be reduced by 30%. The mechanical parts for the induction cells are, however, identical and the cost reduction will apply to about 300 units rather than 100. However, the costs for the mechanical parts were derived from the Los Alamos DARHT accelerator which built 88 cells of the type shown on Fig. 19, the cost reduction will apply only to the additional 200 units.

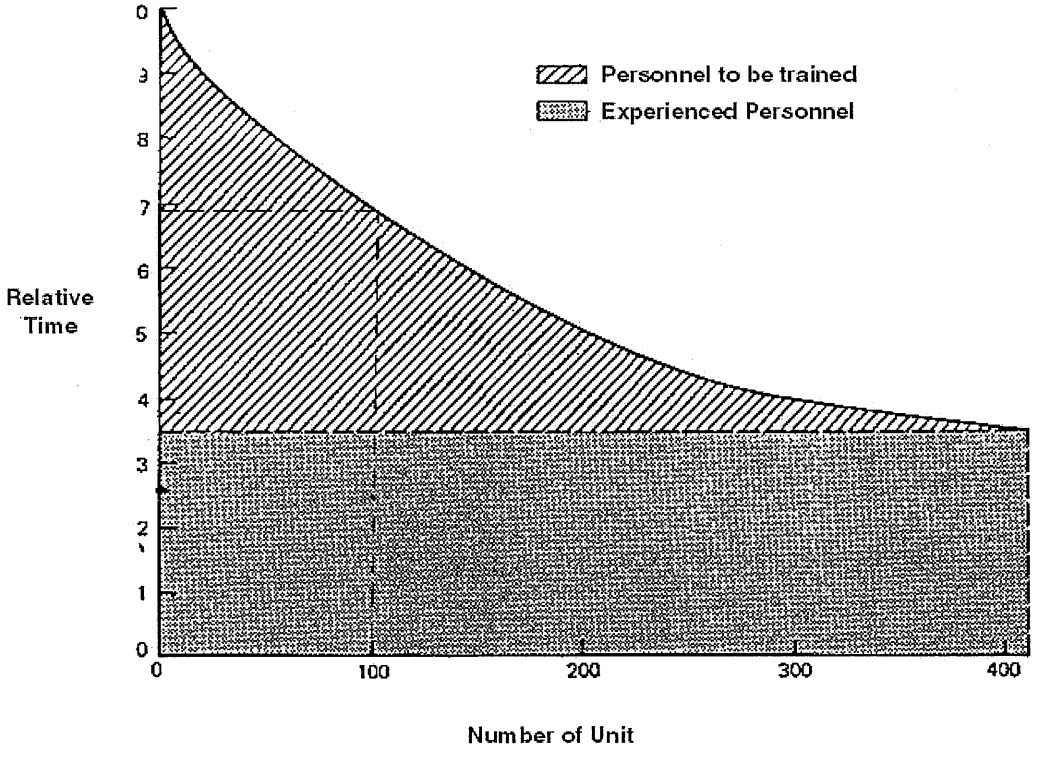

Fig.18-Learning Curve or Relative Time Reduction for Large Quantities.

The cost of materials such as thyratrons, capacitors magnetic materials and other components are expected to follow similar curves. It is important to apply the price reduction from the appropriate starting point. In most cases for the Induction 1, 2 and 3, the starting point was another similar accelerator such as DARHT or the ETAII so the starting point for different components and the learning curve varied.

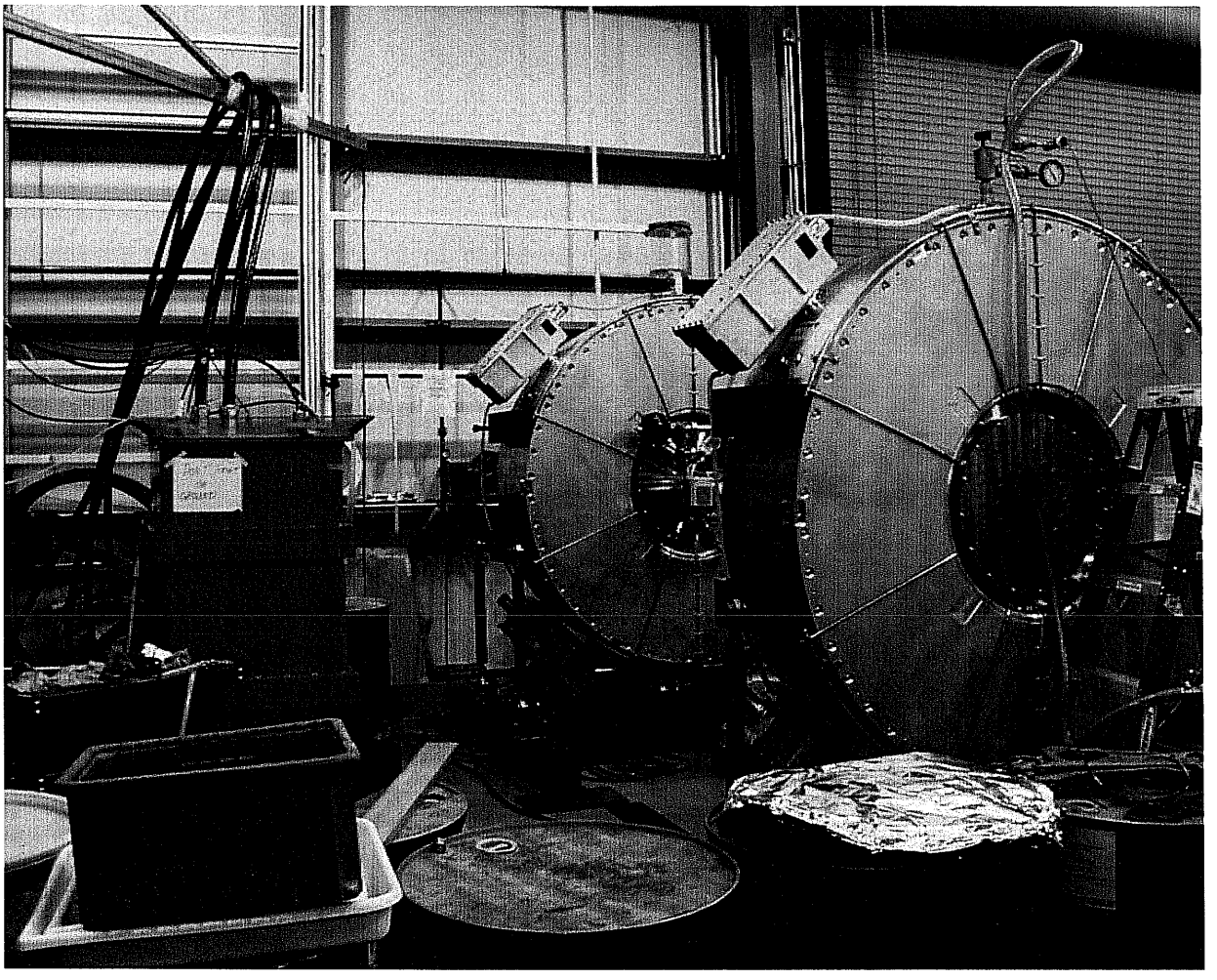

Fig. 19-Dual Axis Radiographic HydroTest (DARHT) Accelerator, Cells.

APPENDIX B

Branched Magnetics to combined Induction 1 and 2.

A technology which has been proposed for ultra high repetition rate systems, should be investigated since it would allow us to go back to two induction accelerators by driving them with a bipolar pulse using the technique of branched magnetics. Fig. 20 shows the schematic for generating an eight pulse burst by magnetic pulse compression and summing. The idea would be to apply this technique by combining the pulsers

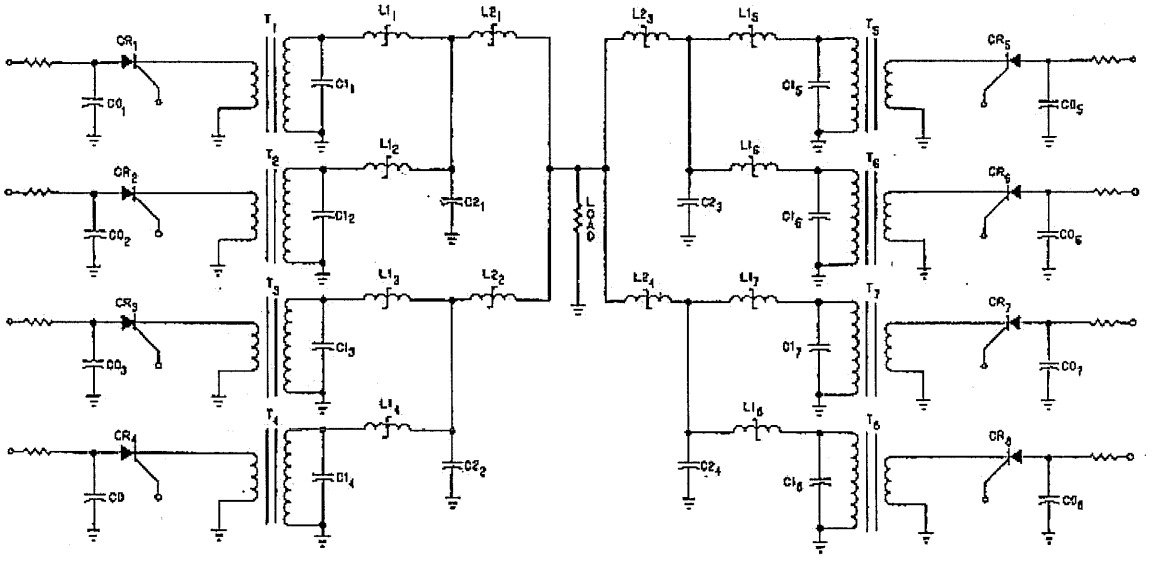

Fig.20- The Concept of branched magnetics.

for induction 2 and 3 and eliminating the induction cells (not the transport) of Induction 3. The pulse generators for Induction 2 and 3 may increase in cost due to the additional magnetics for the summing but it would eliminate the need for 80 accelerator cells. If one assumes a 10% increase in the pulse generators, then the net savings if one were to apply this technique would be about 22M$. This is definitely the riskier approach and would require considerable more development, prior to adopting it.

APPENDIX C

Development and Prototyping

If a serious effort is to be undertaken beyond the study stages, then prototyping of all the major components should be started. Negotiation with Honeywell (Allied Signal) scientists are ongoing in trying to achieve less lossy (thinner) amorphous alloys at even lower prices than the DARHT accelerator. Since the losses go inversely as the ribbon thickness squared, then in going from a ribbon thickness 20.3μm to 18μm would result in a 20% savings in power or about 1.7MW.

The induction cells and the magnetic pulse compression system for driving seven cells should be constructed and tested.

The branched magnetics should also be developed and tested since it also could result in about 20M$ in savings.

A magnetic materials testing program should also be initiated since it could also yield lower losses, hence, lower power requirements.

The superconducting solenoid has dictated the design of this very large ID induction accelerator. The stray fields and their effects on the magnetic material should be investigated since there is great potential for energy and cost savings by reducing the inside diameter (ID).